

引用格式: MA Qiqi, FENG Zhongyao, WANG Ruohui, et al. Research on Soil Heat Transfer with Distributed Optical Fiber Sensing for Pipeline Monitoring[J]. Acta Photonica Sinica, 2023, 52(6):0606002

马琦琦,冯忠耀,王若晖,等.面向管线监测的分布式光纤传感土壤传热研究[J].光子学报,2023,52(6):0606002

# 面向管线监测的分布式光纤传感土壤传热研究

马琦琦<sup>1,2</sup>,冯忠耀<sup>1,2</sup>,王若晖<sup>1,2</sup>,乔学光<sup>1,2</sup>

(1 西北大学 物理学院, 西安 710127)

(2 西北大学 油气资源光纤测井技术陕西省高校工程研究中心, 西安 710127)

**摘要:**现存的管道泄漏监测技术空间分辨率有限,且常规的光纤布置方式难以达到所要求的分辨率。基于此,针对油气管线监测布线问题,在一维平铺式线监测的基础上,提出了正弦式表面监测的光纤铺设方式。以高空间分辨率的光频域反射分布式光纤传感技术为辅助手段,验证了正弦式光纤铺设方法的优越性,其能够全面地反映土壤整个面的温度分布,监测范围变广,漏检可能性降低。采用变量法分析了土壤容重、土壤含水率与土壤导热系数之间的关系以及热源温度对土壤传热的影响,验证了光频域反射分布式光纤传感技术能够精确地监测土壤温度场,并利用土壤温度场的变化规律为其他分布式测温技术在埋地光纤布置时提供指导。

**关键词:**光纤传感;光频域反射;温度测量;正弦式光纤铺设方式;土壤导热系数;土壤含水率

中图分类号:O43

文献标识码:A

doi:10.3788/gzxb20235206.0606002

## 0 引言

油气管道输送在能源分配中发挥着重要作用,埋地管道具有隐蔽性,当泄漏发生时通常会引引起温度、压力、振动等信号的变化,探测信号变化的方法主要有负压波法<sup>[1]</sup>、红外热成像法<sup>[2]</sup>和人工巡视法<sup>[3]</sup>等,这些监测方法有各自的盲区,比如单点监测、测量精度低、存在电磁干扰。温度监测方法<sup>[4]</sup>由于信号容易被监测,且无其他干扰,已经得到广泛应用,为土壤温度场实验研究提供了理论参考。

光纤测温技术<sup>[5]</sup>的快速发展为监测油气管道泄漏引起土壤温度场的变化带来了新方向<sup>[6]</sup>,与传统技术相比,光纤传感技术具有抗电磁干扰、精度高、响应时间快、适用性强、成本低等优点<sup>[7]</sup>,大量学者对管道泄漏引起的土壤温度场分布进行了研究。刘洪飞<sup>[8]</sup>基于光纤拉曼散射的分布式测温技术搭建了埋地管道泄漏试验模型,研究了传输物质温度、泄漏流量等因素对监测的影响,使得泄漏判断和定位更加全面和准确。HEDAYATI-DEZFOOLI M<sup>[9]</sup>利用 T-TDR 型号探头研究了不同温度下土壤单元在稳态条件下的温度分布,为非稳态条件下土壤温度场监测提供参考。周志明等<sup>[10]</sup>将 Peng-Robinson 真实气体状态方程、拉曼光时域反射仪和有限元法相结合,模拟分析了高压埋地天然气管道泄漏区域的温度分布。王正江、王红义<sup>[11]</sup>基于分布式光纤测温技术建立了恒温气团模型,估算了热影响范围和温度分布,为布置光纤提供了参考。这些研究仅考虑了管道泄漏后气体对土壤温度变化的影响,没有考虑到土壤内部物理特性对温度变化的影响。土壤是三相复杂系统,其热物性参数随土壤种类、孔隙率和温湿度改变而改变<sup>[12]</sup>,因此研究土壤内部传热对管道泄漏监测有重要意义。目前试验中使用的土壤传热模型比例通常较小,这需要分布式光纤温度监测具有较高的精度和空间分辨率<sup>[13]</sup>。在如今发展的光纤传感技术类型中,光纤布拉格光栅传感技术<sup>[14]</sup>、布里渊光时域反射计<sup>[15]</sup>和分布式光纤测温技术的空间分辨率有限,不能满足微小泄漏引起的土壤温度场监测。光频域反射(Optical Frequency Domain Reflectometry, OFDR)技术是分布式光纤传感技术中新崛起的

基金项目:国家自然科学基金(Nos. 61735014, 61927812)

第一作者:马琦琦,Email:maqiqi@stumail.nwu.edu.cn

通讯作者:冯忠耀,Email:fengzhongyao@nwu.edu.cn

收稿日期:2022-12-12;录用日期:2023-02-20

<http://www.photon.ac.cn>

方向,具有信噪比高、空间分辨率高、定位准确等优点<sup>[16]</sup>,已广泛应用于光纤参数传感,尤其是温度和应变,因此,OFDR技术在土壤温度场研究中具有很大的潜力。另外,由于监测设备空间分辨率较低无法达到测量需求,诸多专家针对改善设备的空间分辨率进行了研究,大多是通过多种传感器混合使用或者改善硬件来提升空间分辨率<sup>[17]</sup>,在实际应用中,硬件设施的空间分辨率是固定的,只能调整光纤的布置方式。国内外针对光纤的布置方式并没有进行系统的研究,常规光纤的敷设方法大多是沿着被测对象按一维方向敷设,光纤平放于沟底以释放光纤应力,但只适用于监测沿线温度,对于被测对象表面较大和监测要求空间分辨率较高时,这种一维敷设方式难以达到所要求的分辨率,亟需对其进行优化。

针对油气管线监测布线问题,在常规一维平铺式线监测的基础上提出了正弦式面监测光纤铺设方法,并通过OFDR分布式光纤传感技术作为辅助手段验证该敷设方式监测土壤温度的可行性,将该方式应用于土壤传热测量,能够实时准确地监测土壤温度分布面情况。

## 1 OFDR土壤温度场测量系统

### 1.1 实验装置

图1为实验装置,该装置包括实验沙箱、加热模块和数据采集系统三部分。使用耐高温隔热保温涂料对沙箱内部进行隔热保温,加热装置是一个长为4 cm,直径2 mm的圆柱陶瓷电加热探头,放置在沙箱的中间,其加热功率通过线性直流稳压电源进行控制。试验中使用的数据采集系统OFDR反射仪是LUNA公司的OBR4600,该仪器空间分辨率为10 m,能够实现温度和应变测试,在短时间内快速获取所需参数。考虑到裸光纤温度测量过程中可能受到应力作用<sup>[18]</sup>,利用抗压性好的铠装套管对光纤进行松套保护以消除应变干扰,铠装套管具有良好的导热性<sup>[19]</sup>。

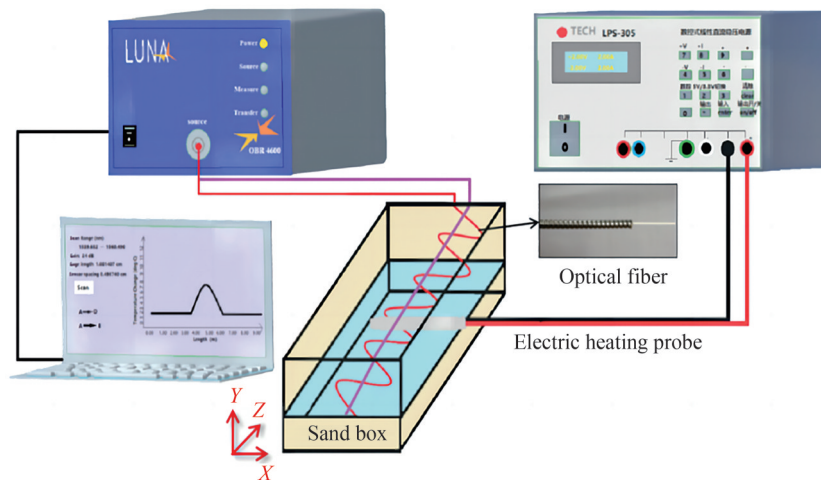


图1 实验装置示意图

Fig. 1 Diagram of the experimental setup

实验目的是通过复杂的光纤敷设方式并利用OFDR技术监测土壤内部温度场的变化情况,确定土壤的传热特性。将试验结果和数值模拟相比较,验证正弦式光纤敷设方式用于土壤传热研究的可行性。实验初始时刻,土壤干燥且无加热,定期扫描光纤温度,以保证多次扫描后光纤的温度趋于稳定,此时光纤的温度作为土壤的初始参考温度,扫描时间间隔为5 min,记录不同实验环境下不同时间埋地光纤的温度。

### 1.2 OFDR技术温度测量原理

OFDR技术是基于光纤中瑞利散射的背向反射技术<sup>[20]</sup>,其技术原理如图2所示。扫频源发射的光进入耦合器中分为两路,一路作为探测光进入光纤,在光纤各个位置点发生瑞利散射,散射光背向传输与另一路参考光在耦合器内相互干涉产生拍频信号,产生的拍频信号被探测器检测到,最后经过采集后可以在计算机中对拍频信号进行分析处理,将频域信号转换到距离域,可得到光纤上各位置处背向反射光的信息,在不考虑相位噪声情况下拍频与待测光纤位置成正比<sup>[21]</sup>。

当温度、压力等外界因素作用于待测光纤某一位置时,瑞利散射频移会在此位置点产生,通过测量瑞利

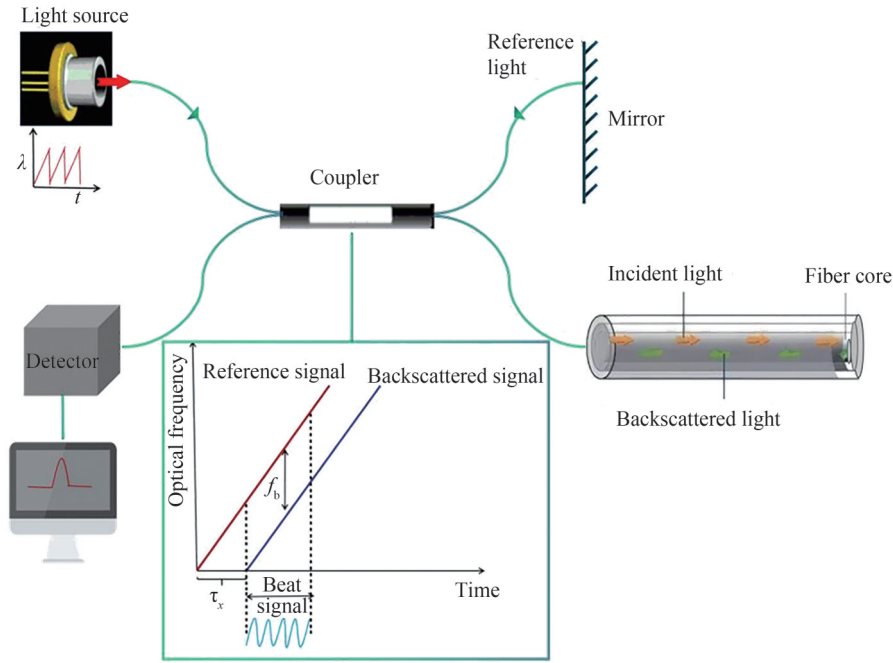


图2 OFDR技术原理

Fig. 2 Principle diagram of the OFDR technology

散射频移量,可以得出该位置的应变和温度<sup>[22]</sup>。比较应力、温度变化前后的瑞利散射光谱飘离零点位置的程度,飘离量对应瑞利散射光谱漂移量<sup>[23]</sup>,瑞利散射频移与应力、温度的关系可以描述为

$$\frac{\Delta\lambda}{\lambda} = K_\epsilon \epsilon + K_T T \quad (1)$$

式中, $\lambda$ 为信号光的波长, $\Delta\lambda$ 为波长的变化量, $K_\epsilon$ 为应力系数, $K_T$ 为总的热系数, $\epsilon$ 为应变值, $T$ 为光纤温度。光纤位置的确定由迈克尔逊干涉仪原理可知,即

$$\tau_x = \frac{2Xn}{c} \quad (2)$$

式中, $\tau_x$ 为反射点时延, $X$ 为光纤散射点, $n$ 为光纤有效折射率, $c$ 为光在真空中的速度。设可调谐光源的线性调谐速率为 $\gamma$ ,则位置 $X$ 对应的光频 $f_b$ 为

$$f_b = \tau_x \gamma \quad (3)$$

由此可见,光频与反射点位间存在线性正比关系,因进入光纤中的光是双程的,最终位置要减半<sup>[24]</sup>,故定位为

$$X = \frac{cf_b}{2n\gamma} \quad (4)$$

## 2 土壤温度场数值模拟

采用瞬态解法<sup>[25]</sup>,利用Comsol模拟仿真软件建立土壤传热模型。该模型由线性热源和三维空间中的土壤组成,计算所需的参数如表1所示。根据室内的研究条件,对传热模型做如下假设:1)土壤的初始温度相同且均匀分布;2)地表温度保持不变,其影响可忽略。数值模拟结果如图3所示,温度从中心呈辐射状向

表1 数值模拟的计算参数

Table 1 Computational parameters for the numerical simulation

Parameter	Value	Parameter	Value
Soil range	1 m × 0.5 m × 0.5 m	Porosity	0.45
Soil density	1 800 kg/m <sup>3</sup>	Heat-up time	120 min
Initial temperature	20 °C	Specific heat capacity	0.92 × 10 <sup>3</sup> J/(kg·°C)

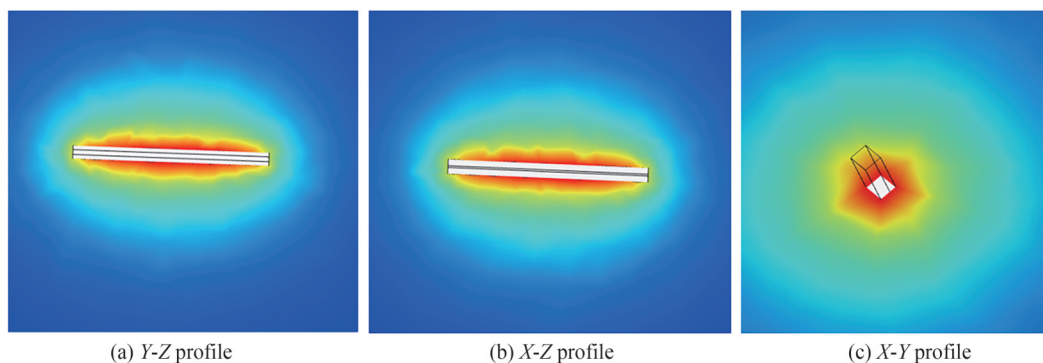


图3 不同剖面的温度云图  
Fig. 3 Temperature clouds of different profiles

四周扩散,等温线越来越稀疏,沿着热源轴向的两个剖面温度分布呈椭圆状,垂直热源的剖面温度分布呈圆形,故热源周围的温度整体呈椭球体。

### 3 光纤敷设方式研究

在分布式管道监测中,不管是工程应用还是实验室研究普遍采用一维平铺的光纤敷设方式。但在实际情况下,管道的任何方向都可能发生泄漏,采用一维平铺式存在漏检的可能,在偏离漏点的各个位置可能没有温度响应或者监测效果差。因此,在一维平铺式基础上提出正弦式光纤敷设方式以避免漏检。

试验准备时期验证了OFDR分布式光纤测温技术的准确性,由于OBR4600反射仪的空间分辨率为 $10\ \mu\text{m}$ ,温度计探头直径为 $2\ \text{mm}$ ,故将分布式光纤长度 $2\ \text{mm}$ 内的温度值取平均值并与同一位置处温度计的示数进行比较,如图4所示,结果表明温度计和分布式光纤测量同一位置的温度基本一致,测量误差小于 $0.5\%$ 。用分布式光纤能够实现温度准确测量。

光纤按照平铺式和正弦式的方式布置在土壤中,正弦式敷设过程中需注意弯曲程度必须在弯曲半径规定的范围内,光纤的弯曲半径应至少为光纤外径的15倍,在施工过程中应至少为20倍,正弦周期与纵向长度分别为 $2\ \text{cm}$ 和 $4\ \text{cm}$ 时光纤的弯曲程度不符合实验要求,故实验中选择正弦周期和纵向长度分别是 $6\ \text{cm}$ 来铺设光纤。图5为土壤垂直距离的温度云图,一维平铺式只能监测到沿线的土壤温度,对于没有铺设到光纤的区域无法监测到温度变化,正弦式能够监测到所覆盖面的土壤温度,监测到的温度呈对称性,提高了监测范围。此外,图6表明试验结果与数值模拟的温度变化趋势相一致,加热初始时刻土壤温度快速上升,加热时间越久,热影响范围显著增大,温度缓慢增长,最后在一段时间后趋于稳定。距离热源 $7\ \text{cm}$ 处温度为 $20.58\ ^\circ\text{C}$ ,与土壤初始温度相差 $0.58\ ^\circ\text{C}$ 且大于系统的温度分辨率 $0.1\ ^\circ\text{C}$ ,可以监测到温度变化。当影响半径在 $7\ \text{cm}$ 以上时,土壤温度基本等于初始温度,无法监测到温度变化,可知光纤与热源之间的布置距离应小于 $7\ \text{cm}$ 。

正弦式布线较复杂,需要考虑正弦的周期与纵向

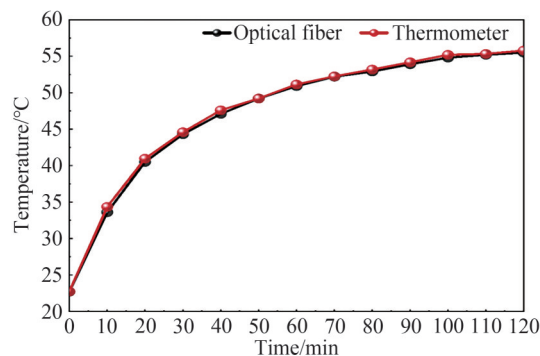


图4 温度计和光纤的温度曲线  
Fig. 4 Temperature curves of thermometer and optical fiber

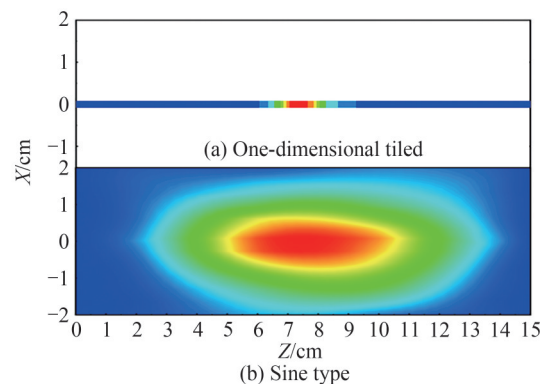


图5 不同敷设方式的温度云图  
Fig. 5 Temperature clouds of different laying methods



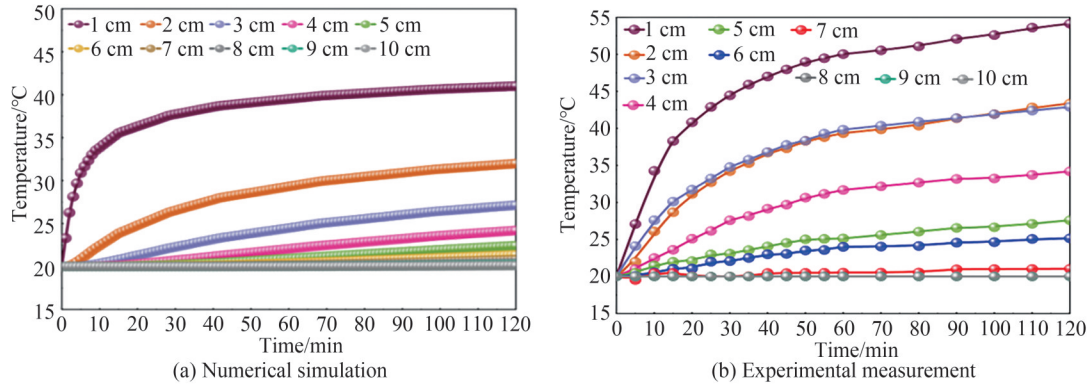
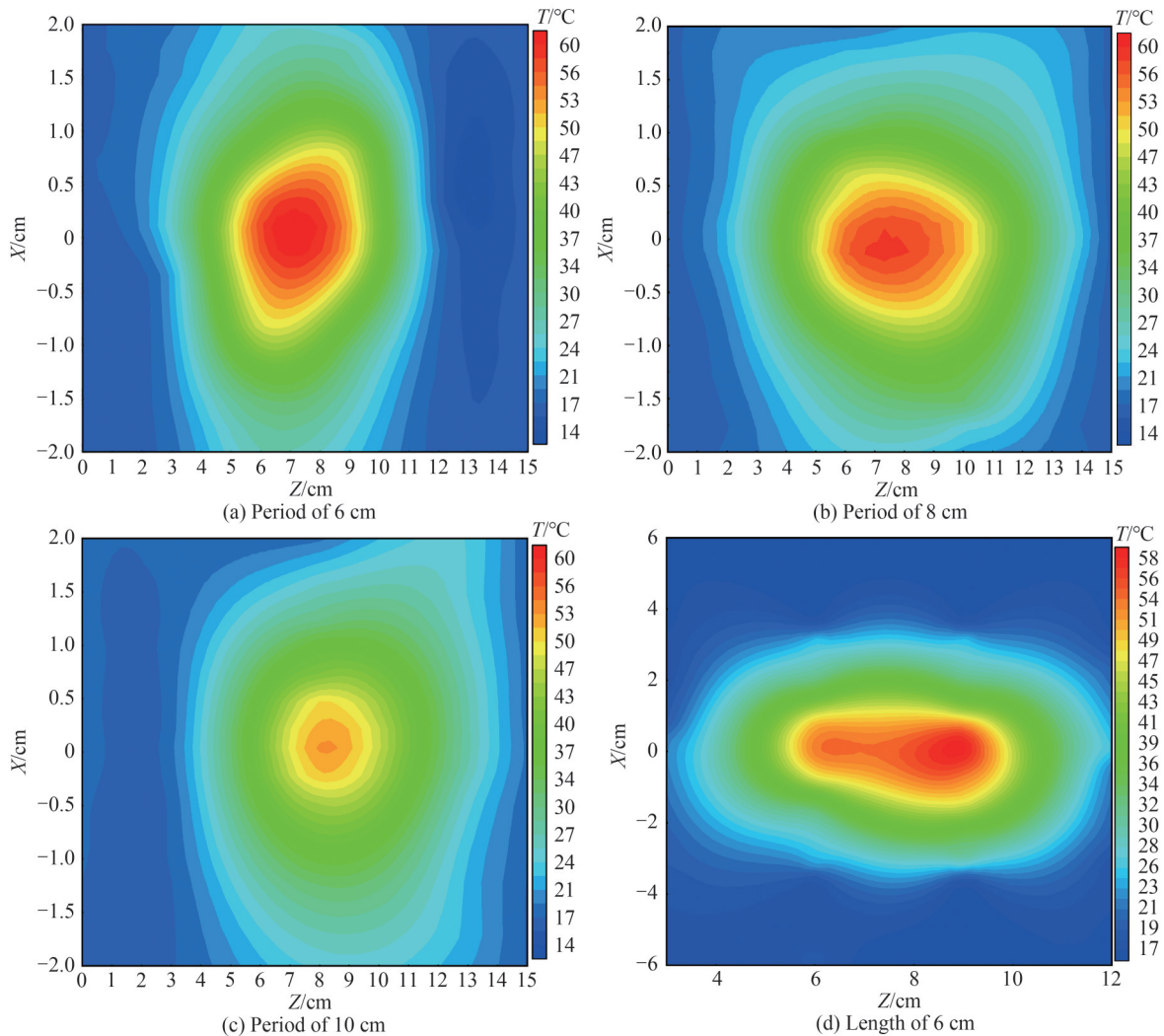


图6 不同影响半径的温度曲线

Fig. 6 Temperature curve of different influence radius

长度,采用控制变量法分别对正弦周期与纵向长度进行分析,范围6~10 cm,对光纤敷设再次进行优化。图7为不同正弦周期和纵向长度下X-Z切面的温度分布,结果表明随着正弦周期和纵向长度从6 cm增加到10 cm,监测到的最高温度从60 °C减小到53 °C,呈降低趋势,热影响范围增大,高温影响范围变小。因此,在高精度监测时布置光纤应在不产生弯曲损耗的情况下紧密排布,比如两者皆为6 cm,若无精度要求建议布置疏松且纵向长度较长,如10 cm左右,这样不仅能监测到所需温度信号还能够避免当泄漏源不在中心正对方向而出现漏检的可能。



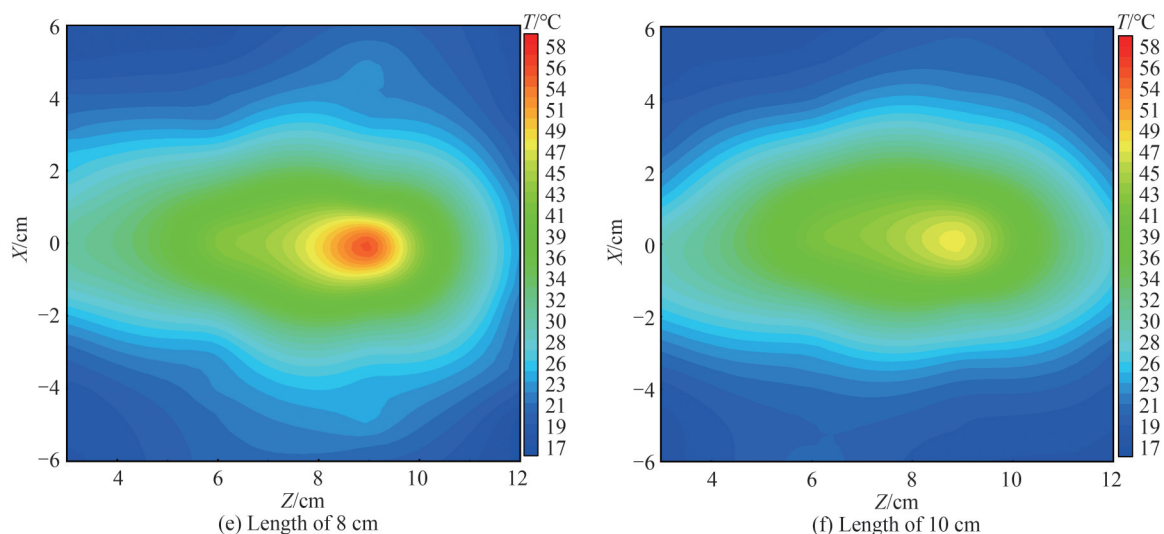


图7 不同条件下X-Z切面温度分布

Fig. 7 Temperature distribution in X-Z section under different conditions

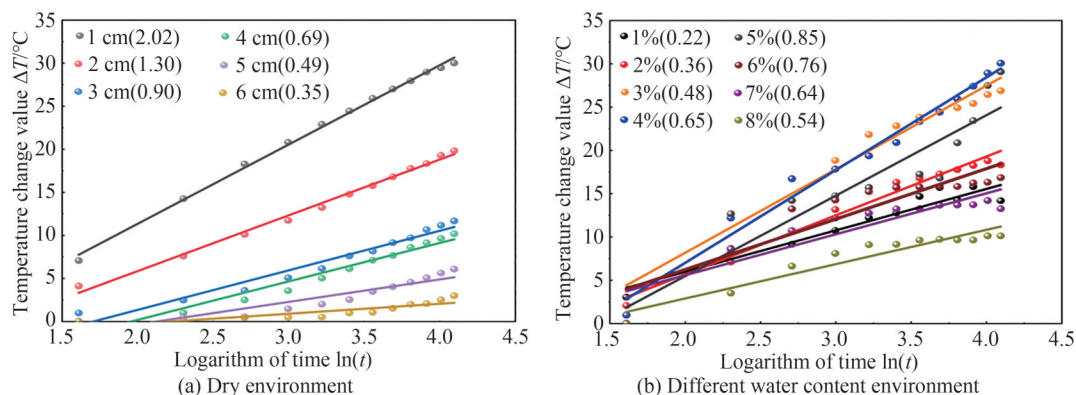
#### 4 分布式光纤监测土壤传热

土壤传热过程很复杂,包括两个过程:一是通过颗粒间空气或水传导;二是通过各颗粒间接触传导<sup>[26]</sup>。土壤导热系数用来表示传导土壤热量的强度,直接影响土体中热流的传播速度和温度场的分布<sup>[27]</sup>,其主要受土壤含水率、干容重、温度等因素影响。采用正弦式光纤敷设方式进行布线,为准确监测到土壤的传热情况,正弦式周期和纵向长度分别选择6 cm,加热功率为4 W,加热时间为120 min,并利用OFDR分布式光纤传感技术测量干燥环境下不同土壤深度的温度,同时测量不同含水率下(1%~8%)的温度。在实验中,将称量好的土壤样品放于沙箱内,加水进行充分混合后,需静止数十个小时才能进行温度测量,以保证土壤内的水分均匀分布。

土壤导热系数公式为<sup>[28]</sup>

$$\Delta T_{\pi} = \frac{q}{4\pi\zeta} \ln \frac{t_2}{t_1} \quad (5)$$

式中, $\Delta T_{\pi}$ 为温度变化值, $q$ 为加热探头的热流量, $\zeta$ 为土壤导热系数, $t_1$ 和 $t_2$ 为不同加热时间。对光纤测量温度变化值 $\Delta T$ 与时间对数 $\ln(t)$ 做线性拟合(图8),通过直线的斜率 $k$ 可计算土壤导热系数 $\lambda$ 。由计算结果分析出土壤导热系数与土壤含水率、土壤容重的关系,为埋地管道的光纤监测研究提供参考。

图8 不同条件下温度变化值 $\Delta T$ 与时间对数 $\ln(t)$ 的拟合曲线Fig. 8 The fitting curve of temperature change  $\Delta T$  and logarithm of time  $\ln(t)$  under different conditions

由土壤深度与土壤容重的关系 $y = 1.11x^{0.06}$ <sup>[29]</sup>得到的土壤容重与土壤导热系数之间关系如图9(a)所示。结果表明计算得到的土壤导热系数在规定的标准范围内和允许的计算误差内与实际值基本重合,同时土壤导热系数随土壤容重的增大呈指数形式增大。因为土壤容重增加使得土壤中空气越来越少,固体颗粒增

多,当土壤容重再次增加时,颗粒间孔隙几乎成为微孔隙,固体间的接触增加,热传导能力增强。图9(b)表明土壤导热系数与含水率之间的关系并不是特定的线性增长趋势或减小趋势,而是随着外界因素的影响呈类抛物线形式变化,含水率低于阈值时土壤导热系数线性增加,反之土壤导热系数呈线性降低趋势。另外,土壤导热率影响着温度的垂直分布<sup>[30]</sup>,含水率对土壤温度的垂直分布也具有影响。选取四种不同含水率(2%、4%、6%、8%)来分析对土壤温度垂直分布的影响。图10表明含水率低于阈值时,随着含水率的增加

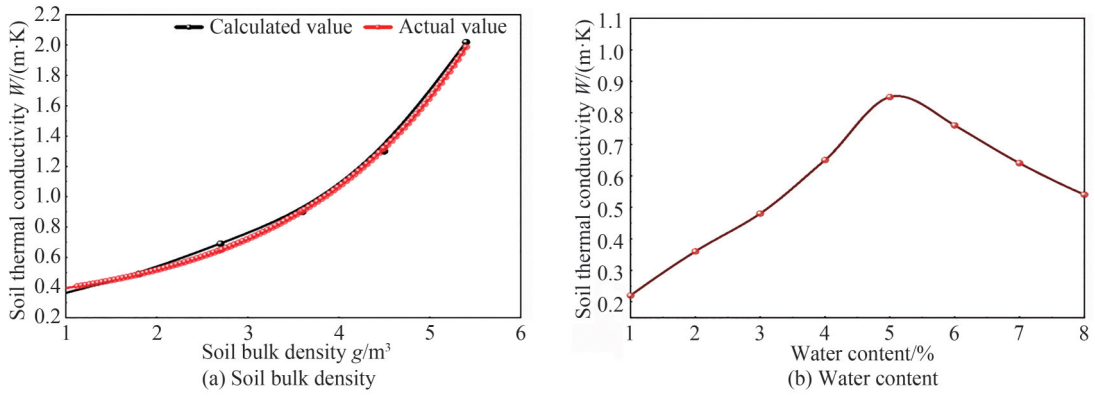


图9 土壤导热系数随土壤容重、含水率的变化

Fig. 9 Variation curve of soil thermal conductivity with soil bulk density and water content

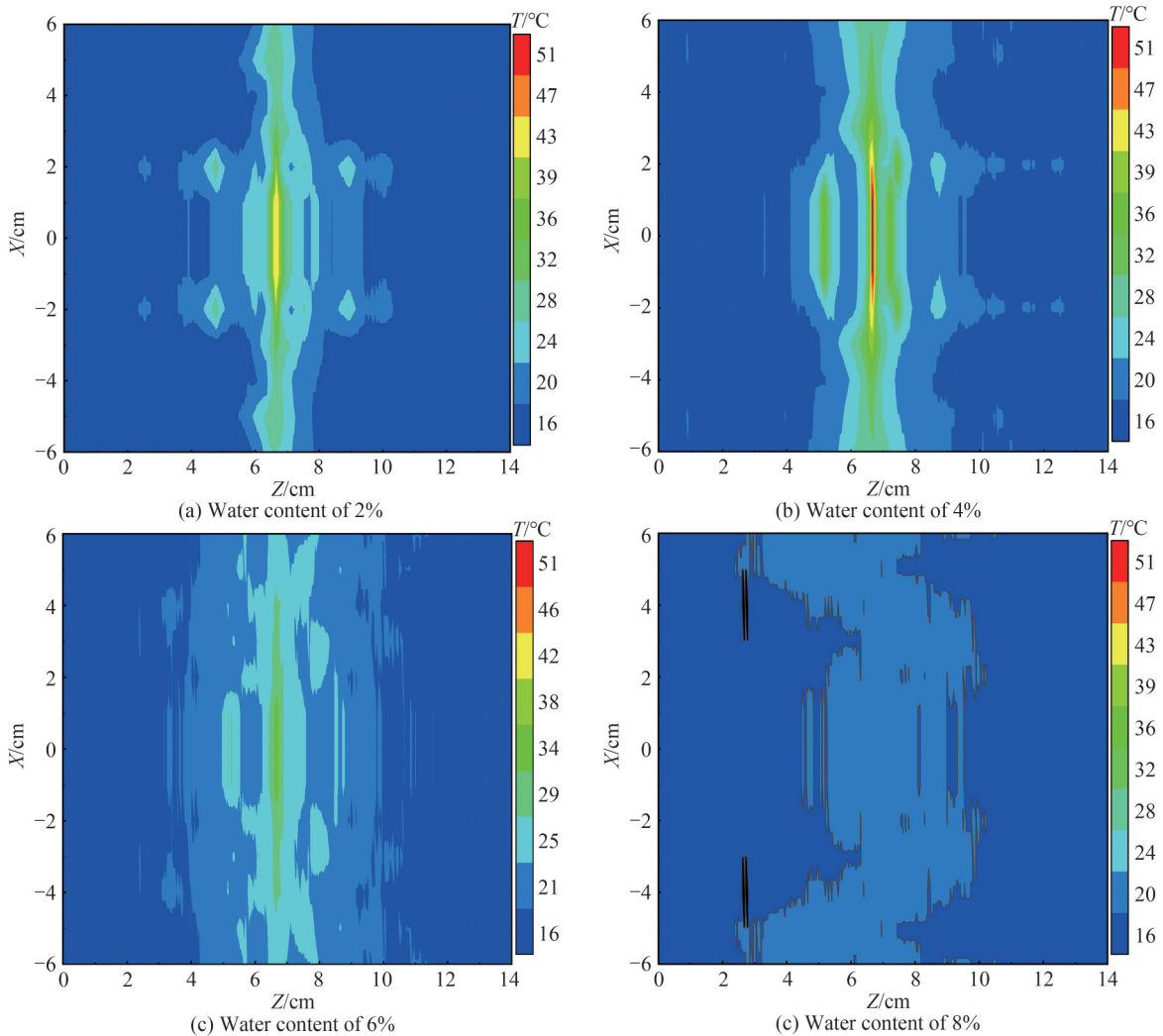


图10 不同含水量下Y-Z切面温度分布

Fig. 10 Temperature distribution in Y-Z section under different water content



垂直方向上土壤传热速度变快,热源周围温度提升变快,监测到的最高温度越大,高温影响范围变大,热扩散程度明显增加。反之,垂直方向的整体温度降低,土壤传热变慢,温度上升速率变慢,高温影响范围缩小,水分过多时温度基本上与土壤初始温度相同。因为含水率较少时固体颗粒与水联系形成水膜,水膜与土壤颗粒之间存在引力,颗粒间距离缩短,接触热阻减小。此外水良好的导热性质,土壤各颗粒间通过水产生联系,增加了热传导的通道,导热系数迅速增大,垂直距离温度扩散得越快,高温范围越大。当水分增加到阈值时,颗粒间由水膜变成联通水,颗粒受水的表面张力作用减小或消失,颗粒间距离重新增大,土壤中的水分接近饱和使土壤导热系数逐渐降低,垂直距离温度扩散得越慢,高温范围越小。因此含水率对土壤导热系数和土壤温度的垂直分布具有促进和抑制双重作用。

热源温度也是土壤传热影响因素之一。在其他实验条件不变的情况下,通过改变加热功率来研究热源温度对土壤传热的影响,为光纤敷设位置进一步提供参考。加热功率分别为4 W、7 W、9 W,土壤初始温度为17.7 °C,以土壤垂直方向为指标,其温度分布如图11所示。结果发现随着热源温度的增加,热扩散范围越大,高温影响范围变大,垂直方向上的温度变化梯度越大,温度传递的距离越远。

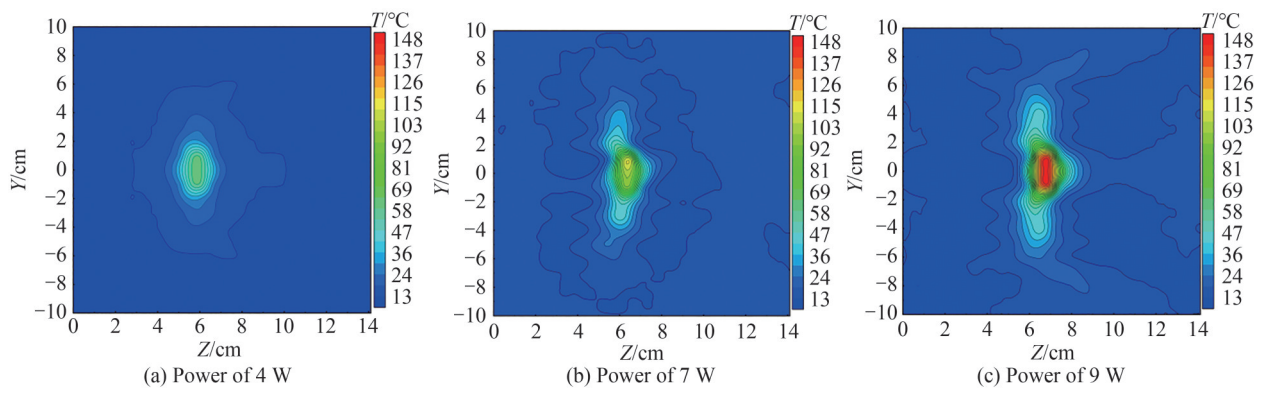


图11 不同功率下土壤温度的垂直分布

Fig. 11 Vertical distribution of soil temperature under different power

## 5 结论

本文利用OFDR分布式光纤传感技术,研究了埋地光纤的布线方式及土壤内部物理特性对土壤传热的影响。结果表明,埋地光纤的正弦式敷设比一维平铺式敷设更加利于温度信号监测,其测量结果优于一维平铺式,从线监测到面监测使得监测范围变广,漏检的可能性降低。土壤中温度以辐射状从中心向四周呈降低趋势扩散,热源轴向温度场呈椭圆形分布,纵向温度场呈圆形分布。通过研究土壤内部物理特性发现土壤容重和含水率对土壤传热的影响巨大,间接影响到实验所监测的温度信号,土壤内部物理特性对土壤传热的影响为光纤布置提供了进一步指导,也为埋地管道泄漏监测提供参考,并且基于OFDR分布式光纤技术高分辨率和高精度的优势,展示了准确全面的土壤温度场分布情况。

### 参考文献

- [1] ZHANG Wei. Discussion on the leakage monitoring and quasi-real-time detection of long-distance oil pipeline[J]. China Petroleum and Chemical Standards and Quality, 2021, 41(6):63-65.  
张威. 长距离输油气管道泄漏监测与准实时检测技术及应用问题探讨[J]. 中国石油和化工标准与质量, 2021, 41(6): 63-65.
- [2] LI Zheng. Discussion on the operation monitoring and leakage detection technology of directly buried heating pipeline[J]. District Heating, 2016(5): 125-127+131.  
李征. 直埋供热管道运行监测与泄漏检测技术探讨[J]. 区域供热, 2016(5): 125-127+131.
- [3] SAKAKI T, TSUGAWA R. Effects of heat source conditions on the early temperature rise in heated fiber-optic cable emplaced in granulated bentonite mixture[J]. Geomechanics for Energy and the Environment, 2021, 28.
- [4] MA Jian, ZHENG Yu, YU Haihu. A temperature and glucose solution concentration sensor based on etched optical fiber [J]. Acta Photonica Sinica, 2017, 46(4): 0406003.  
马健, 郑羽, 余海湖. 基于腐蚀光纤的温度及葡萄糖溶液浓度传感器[J]. 光子学报, 2017, 46(4): 0406003.
- [5] XING Haojian, QIAO Qiuxiao, JIN Zhongxie. Monitoring technology of nuclear power primary circuit leakage point based



- on distributed temperature sensor[J]. *Acta Photonica Sinica*, 2019, 48(5): 0506004.
- 邢豪健, 乔秋晓, 金钟燮. 基于分布式光纤拉曼测温系统的核电一回路泄漏点监测技术[J]. *光子学报*, 2019, 48(5): 0506004.
- [6] ERSON R C, MULLER R S, TOBIAS C W. Investigations of porous silicon for vapor sensing[J]. *Sensors and Actuators A: Physical*, 1990, 23(1-3): 835-839.
- [7] HAN Xiaopeng, LIU Chunyu, ZHAO Chunlong, et al. Optimized double cone structure based on Mach-Zendel interference principle for strain and temperature synchronous sensing[J]. *Acta Photonica Sinica*, 2020, 49(8): 0806004.
- 韩晓鹏, 柳春郁, 赵纯龙, 等. 基于马赫曾德尔干涉原理的优化双锥结构应变温度同步传感[J]. *光子学报*, 2020, 49(8): 0806004.
- [8] LIU Hongfei. Research on integrity evaluation method of oil and gas pipeline based on distributed optical fiber sensing[D]. Dalian: Dalian University of Technology, 2018.
- 刘洪飞. 基于分布式光纤传感的油气管道完整性评价方法研究[D]. 大连: 大连理工大学, 2018.
- [9] HEDAYAT T D Z FOOLI M, LEONG W H. An experimental study of coupled heat and moisture transfer in soils at high temperature conditions for a medium coarse soil[J]. *International Journal of Heat and Mass Transfer*, 2019, 137: 18.
- [10] ZHOU Zhaoming, ZHANG Jia, HUANG Xuesong, et al. Experimental study on distributed optical-fiber cable for high-pressure buried natural gas pipeline leakage monitoring[J]. *Optical Fiber Technology*, 2019, 53(C): 102028.
- [11] WANG Jiangwei, WANG Hongyi. Effects of natural gas pipeline leaks on surrounding soil temperatures[J]. *Petroleum Engineering Construction*, 2020, 46(2): 5-8.
- 王江伟, 王红义. 天然气管道泄漏对周围土壤温度的影响[J]. *石油工程建设*, 2020, 46(2): 5-8.
- [12] LIN Gang, SHANG Yongbin, YANG Lilei, et al. Study on the distribution pattern of soil temperature field along buried liquid CO<sub>2</sub> pipeline[J]. *Petroleum Engineering Construction*, 2018, 44(4): 13-18, 24.
- 林罡, 商永滨, 杨立雷, 等. 埋地液态CO<sub>2</sub>管道沿线土壤温度场分布规律研究[J]. *石油工程建设*, 2018, 44(4): 13-18, 24.
- [13] LU Sen, REN Tusheng, ROBERT H. Estimating the components of apparent thermal conductivity of soils at various water contents and temperatures [J]. *Geoderma*, 2020, 376(1): 114530.
- [14] YU Haihu, MA Yue, GAO Wenjing, et al. Preparation of dense tapered fiber grating arrays and experimental study of their quasi-distributed temperature sensing[J]. *Acta Photonica Sinica*, 2021, 50(7): 0706001.
- 余海湖, 马悦, 高文静, 等. 密集切趾光纤光栅阵列制备及其准分布式温度传感的实验研究[J]. *光子学报*, 2021, 50(7): 0706001.
- [15] LI Shiyi, LI Hao, JI Wenbin, et al. Optical fiber sensing structure for slope monitoring based on Brillouin optical time domain reflectometer[J]. *Acta Photonica Sinica*, 2021, 50(9): 0906005.
- 李时宜, 李浩, 季文斌, 等. 基于布里渊光时域反射仪的边坡监测光纤传感器结构[J]. *光子学报*, 2021, 50(9): 0906005.
- [16] SUO Liujia. Study on distributed fiber optical strain demodulation method based on OFDR[D]. Dalian: Dalian University of Technology, 2019.
- 锁刘佳. 基于OFDR的分布式光纤应变解调方法研究[D]. 大连: 大连理工大学, 2019.
- [17] SCHENATO L, PALMIERI L, CAMPORESE M, et al. Distributed optical fibre sensing for early detection of shallow landslides triggering[J]. *Scientific Reports*, 2017, 7(1): 28.
- [18] CHEN Lin, ZHANG Anan, CAO Buliang, et al. An experimental study on monitoring the phreatic line of an embankment dam based on temperature detection by OFDR[J]. *Optical Fiber Technology*, 2021, 63(63): 102510.
- [19] WANG Rong, YANG Chenlei, NI Long, et al. Experimental study on heat transfer of soil with different moisture contents and seepage for ground source heat pump[J]. *Indoor and Built Environment*, 2020, 29(9): 1238-1248.
- [20] LIANG Changshuo, BAI Qing, YAN Min, et al. A comprehensive study of optical frequency domain reflectometry[J]. *IEEE Access*, 2021, 9: 41647-41668.
- [21] LALAM N, LU Ping, LU Fei, et al. Distributed carbon dioxide sensor based on sol-gel silica coated fiber and Optical Frequency Domain Reflectometry (OFDR)[J]. *Industrial Optical Devices and Systems*, 2020, 11500: 115000M.
- [22] WANG Zichao, LIU Zhiang, YANG Huadong. Optical frequency domain reflection and structural monitoring performance of ultra-weak fiber Bragg grating technology[J]. *Advances in Laser and Optoelectronics*, 2022, 59(21): 105-111.
- 王紫超, 刘志昂, 杨华东. 光频域反射与超弱光纤布拉格光栅技术的结构监测性能[J]. *激光与光电子学进展*, 2022, 59(21): 105-111.
- [23] SOUZA G, TARPANI J R. Distributed fiber optics sensing applied to laminated composites: embedding process, strain field monitoring with OBR and fracture mechanisms[J]. *Journal of Nondestructive Evaluation*, 2020, 39(4): 1-15.
- [24] LEAL J, ARNALDO G, MARQUES C, et al. Viscoelastic features based compensation technique for polymer optical fiber curvature sensors[J]. *Optics and Laser Technology*, 2018, 105: 35-40.

- [25] MCKENZIE J M. Uncertainties in measuring soil moisture content with actively heated fiber-optic distributed temperature sensing[J]. *Sensors*, 2021, 21: 3723.
- [26] ZHOU Zhaoming, HUANG Jia, HUANG Xuesong, et al. Trend of soil temperature during pipeline leakage of high-pressure natural gas: Experimental and numerical study[J]. *Measurement*, 2020, 153(C): 107440.
- [27] ZHU Chuanyong, HE Zhiyang, DU Mu, et al. Predicting the effective thermal conductivity of unfrozen soils with various water contents based on artificial neural network[J]. *Nanotechnology*, 2021, 33(6): 11.
- [28] LU Sen, REN Tusheng. Model for predicting soil thermal conductivity at various temperatures[J]. *Transactions of the Chinese Society of Agricultural Engineering*, 2009, 25(7): 13-18.
- [29] LIU Xiuxiu. Theoretical and experimental study on the diffusion of gas pipeline leakage in comprehensive pipeline corridors [D]. Beijing: Beijing University of Architecture, 2018.  
刘秀秀. 综合管廊燃气管道泄漏扩散理论与实验研究[D]. 北京: 北京建筑大学, 2018.
- [30] ZHOU Yuanyuan, JIANG Haifeng, LI Hui, et al. Experimental study on thermal conductivity of aqueous sandy soil[J]. *Journal of Engineering Thermophysics*, 2015, 36(2): 265-268.  
周媛媛, 江海峰, 李辉, 等. 含水砂土导热系数实验研究[J]. *工程热物理学报*, 2015, 36(2): 265-268.

## Research on Soil Heat Transfer with Distributed Optical Fiber Sensing for Pipeline Monitoring

MA Qiqi<sup>1,2</sup>, FENG Zhongyao<sup>1,2</sup>, WANG Ruohui<sup>1,2</sup>, QIAO Xueguang<sup>1,2</sup>

(1 *School of Physics, Northwest University, Xi'an 710127, China*)

(2 *Engineering Research Center of Optical Fiber Well Logging Technology for Oil and Gas Resources, Universities of Shaanxi Province, Northwest University, Xi'an 710127, China*)

**Abstract:** With the development of petroleum and natural gas resources, pipeline transportation has become one of the main transportation modes. Pipeline leakage caused by various external factors during transportation affects the safe running of the pipeline. The development of optical fiber sensing technology has brought a new solution for pipeline leakage monitoring. Most of the existing research are carried out by numerical simulation work, lacking experimental demonstration, and only studied the temperature field distribution in the soil area after pipeline leakage, without taking the impact of the difference in soil internal physical properties on the temperature change into account. In addition, the accuracy of the monitoring of small leaks still can't satisfy the monitoring requirements. And the conventional fiber arrangement is only suitable for monitoring the temperature along the line, when the surface of the object to be measured is large and the monitoring requires a higher spatial resolution, the one-dimensional laying method is difficult to achieve the required resolution, it needs to be optimized.

Based on the advantages of high spatial resolution of optical frequency domain reflectometry technology, in this paper, we mainly focus on oil and gas pipeline monitoring wiring problem and build a sandbox model with a small proportion. On the basis of one-dimensional tiled line monitoring, a new way of laying optical fiber for sinusoidal surface monitoring is proposed. Using optical frequency domain reflectometry technology with high spatial resolution as a supporting tool, the superiority of sinusoidal layout is verified. The results show that the measurement effect of buried optical fiber with a sinusoidal layout is better than that of a conventional one-dimensional tiled layout because of its wider measurement range. We analyzed the effect of sinusoidal period and longitudinal length on temperature monitoring, these two factors have a greater effect on the monitored maximum temperature, which means the larger the sine period and vertical length, the lower the highest temperature detected. Therefore, if there is no precision requirement, the optical fiber can be arranged long and sparse. Otherwise, it needs to be even tighter. Through the combination of experiments and numerical simulations, it is obtained that the maximum thermal influence radius of the tiny heat source is 7 cm, and this result can further guide to optimize the arrangement of optical fiber. In addition, the relationship between soil thermal conductivity, soil bulk density, and water content is obtained by the variable method. The relationship between soil bulk density and soil thermal conductivity is basically linear, the relationship between soil thermal conductivity and water content is not a specific linear increasing or decreasing trend, it varies in a parabolic-like form with

the influence of external factors. Water content also affects the vertical distribution of the soil temperature field. When the water content is below the threshold, as it increases the rate of soil heat transfer in the vertical direction becomes faster, the temperature around the heat source increases faster, the maximum temperature monitored becomes larger, the high temperature influence range becomes larger, and the degree of heat diffusion increases significantly. We have studied the effect of heat source temperature on soil heat transfer, and found that as the heat source temperature increases, the heat diffusion range becomes larger, the high temperature influence range becomes larger, and the distance of temperature transfer in the vertical direction becomes farther. The influence law of these factors on soil heat transfer provides a reference for pipeline leakage monitoring, which can further guide the fiber arrangement. Meanwhile, it also verifies the feasibility of optical frequency domain reflectometry distributed optical fiber technology can accurately measure soil temperature field and also provides guidance for other distributed temperature measurement technologies in the layout of buried optical fibers.

**Key words:** Optical fiber sensing; Optical frequency domain reflectometry; Temperature measurement; Sinusoidal fiber laying mode; Soil thermal conductivity; Soil water content

**OCIS Codes:** 060.2330; 060.2300; 060.2370; 120.6780